



## Article

# Potential of Sentinel-1 Images for Estimating the Soil Roughness over Bare Agricultural Soils

Nicolas Baghdadi <sup>1,\*</sup> , Mohammad El Hajj <sup>1</sup>, Mohammad Choker <sup>1</sup>, Mehrez Zribi <sup>2</sup> ,  
Hassan Bazzi <sup>1</sup>, Emmanuelle Vaudour <sup>3</sup>, Jean-Marc Gilliot <sup>3</sup> and Dav M. Ebengo <sup>3</sup>

<sup>1</sup> Territoires, Environnement, Télédétection et Information Spatiale (TETIS), Institut National de Recherche en Sciences et Technologies Pour l'Environnement et l'Agriculture (Irstea), University of Montpellier, 500 rue François Breton, 34093 Montpellier CEDEX 5, France; mohammad.el-hajj@teledetection.fr (M.E.H.); mohammad.choker@teledetection.fr (M.C.); bazzihasan1@gmail.com (H.B.)

<sup>2</sup> Centre d'Etudes Spatiales de la Biosphère (CESBIO), Centre National de la Recherche Scientifique (CNRS), 18 av. Edouard Belin, bpi 2801, 31401 Toulouse CEDEX 9, France; mehrez.zribi@ird.fr

<sup>3</sup> Écologie Fonctionnelle et Ecotoxicologie des Agroécosystèmes (ECOSYS), AgroParisTech, Institut National de la Recherche Agronomique (INRA), Université Paris-Saclay, 78850 Thiverval-Grignon, France; emmanuelle.vaudour@agroparistech.fr (E.V.); jean-marc.gilliot@agroparistech.fr (J.-M.G.); dav.ebengomwampongo@agroparistech.fr (D.M.E.)

\* Correspondence: nicolas.baghdadi@teledetection.fr

Received: 13 December 2017; Accepted: 29 January 2018; Published: 31 January 2018

**Abstract:** The purpose of this study is to analyze the potential of Sentinel-1 C-band SAR data in VV polarization for estimating the surface roughness (*Hrms*) over bare agricultural soils. An inversion technique based on Multi-Layer Perceptron neural networks is used. It involves two steps. First, a neural network (NN) is used for estimating the soil moisture without taking into account the soil roughness. Then, a second neural network is used for retrieving the soil roughness when using as an input to the network the soil moisture that was estimated by the first network. The neural networks are trained and validated using simulated datasets generated from the radar backscattering model IEM (Integral Equation Model) with the range of soil moisture and surface roughness encountered in agricultural environments. The inversion approach is then validated using Sentinel-1 images collected over two agricultural study sites, one in France and one in Tunisia. Results show that the use of C-band in VV polarization for estimating the soil roughness does not allow a reliable estimate of the soil roughness. From the synthetic dataset, the achievable accuracy of the *Hrms* estimates is about 0.94 cm when using the soil moisture estimated by the NN built with a priori information on the moisture volumetric content "*mv*" (accuracy of *mv* is about 6 vol. %). In addition, an overestimation of *Hrms* for low *Hrms*-values and an underestimation of *Hrms* for *Hrms* higher than 2 cm are observed. From a real dataset, results show that the accuracy of the estimates of *Hrms* in using the *mv* estimated over a wide area (few km<sup>2</sup>) is similar to that in using the *mv* estimated at the plot scale (RMSE about 0.80 cm).

**Keywords:** Sentinel-1; SAR; C-band; soil; roughness; moisture; Integral Equation Model; neural network

## 1. Introduction

Soil surface characteristics (mainly soil moisture and surface roughness) play a key role in different hydrological processes (floods, runoff, evapotranspiration, infiltration, soil erosion, and imbalance in the water cycle). Surface roughness has a role in trapping water at the surface and reducing flow velocity, which increases infiltration and in turn reduces downstream runoff. The roughness scales observed by a radar sensor have a strong dependence on the frequency and radar incidence [1].

The most commonly used techniques for measuring soil roughness are laser scanner, photogrammetry, and mechanic profilometer. The roughness description is based on the computation of the surface height autocorrelation function from which two parameters are generally calculated. The first is the standard deviation of the surface height (root mean square surface height,  $H_{rms}$ ), defining the vertical scale of the roughness. The second one corresponds to the surface correlation length ( $L$ ) defined as the horizontal displacement for which the correlation function of the profile decreases to  $1/e$ . For 95% of in situ measurements in agricultural areas,  $H_{rms}$  ranges from 0.25 cm for extremely smooth soils to 4 cm for ploughed fields, and the correlation length ranges between 2 and 20 cm [2]. As it is generally very difficult to retrieve  $H_{rms}$  and  $L$  in addition to soil moisture by inverting the backscattered radar signals of current SAR sensors; only  $H_{rms}$  is often used to characterize the soil roughness in the inversion algorithms of SAR signal. In addition, Zribi et al. [3] introduced a new roughness parameter combining  $H_{rms}$ ,  $L$  and the correlation function power ( $\alpha$ ) into a single parameter  $Z_g$ , defined as  $H_{rms} (H_{rms}/L)^\alpha$ . This parameter takes the influence of  $H_{rms}$ .

Numerous studies have shown that radar signal is strongly sensitive to soil roughness in agricultural areas mainly for small  $H_{rms}$ -values [4–9]. In addition, this sensitivity increases with the incidence angle and the wavelength of the radar signal [10,11]. It has been shown that under these conditions, the backscattered signal increases with the root mean square surface height, according to an exponential or logarithmic function (e.g., [5,9]). A comparison between TerraSAR-X, ASAR and PALSAR data reveals a difference of 8 decibels (dB) between the return signals from smooth and rough fields ( $H_{rms}$  between 0.5 and 3 cm) in the L-band (HH-38°), whereas this difference is approximately 4 dB in the C- and X-bands, at an incidence of around 25°, for both HH and VV polarizations [6]. Aubert et al. [4] have shown that the mean difference between the  $\sigma^\circ$  values of the smoothest ( $H_{rms} = 0.7$  cm) and roughest areas ( $H_{rms} = 3$  cm) reached a maximum of 1.9 dB at 25°, and approximately 3.5 dB at 50°, for data in the X-band. Various studies dealing with the dynamic range of radar signals as a function of surface roughness show that it is difficult to discriminate between roughnesses greater than approximately 1, 1.5 and 2 cm in X-, C- and L-band, respectively (e.g., [6]). Concerning the influence of polarization, Holah et al. [12] found that the HH and HV polarizations are more sensitive to surface roughness than the VV polarization.

In the last decades, important scientific activity has been devoted to demonstrate the potential of Synthetic Aperture Radar (SAR) for mapping the moisture content of agricultural areas [13–18]. The possibility of retrieving surface roughness was insufficiently investigated from SAR images [5,9,15]. The new C-band radar satellites Sentinel-1A (launched on 3 April 2014) and Sentinel-1B (launched on 22 April 2016) provide free and open access data for the whole globe with high spatial and temporal resolutions (one image each 6 days at 10 m spatial resolution). These characteristics of Sentinel-1 open new perspectives for an operational soil roughness mapping.

Baghdadi et al. [5] investigated the potential of the first generation of SAR data (ERS-2 and RADARSAT-1) for monitoring roughness states over bare agricultural fields. Results indicate that high incidence angles (about 45°) are more suitable to discriminate various roughness classes (smooth, medium and rough) over bare agricultural fields. An algorithm based on an experimental exponential relationship between the radar backscattering coefficient and the surface roughness (root mean square surface height,  $H_{rms}$ ) independently of the soil moisture was used. Next, Baghdadi et al. [15] developed an approach to estimate soil moisture and surface roughness from C-band polarimetric RADARSAT-2 data based on neural networks (NNs). Results showed that the accuracy of the soil roughness estimates was about 0.5 cm using polarimetric data. The estimation was better for  $H_{rms}$ -values lower than 2 cm than for  $H_{rms}$ -values higher than 2 cm. For higher  $H_{rms}$ , the NNs under-estimate the surface roughness. Moreover, Zribi and Dechambre [9] proposed an approach based on the use of two SAR images acquired at two different incidence angles, one image with a weak incidence (~20°) and one image with a strong incidence (~40°) for estimating both soil moisture and surface roughness. The surface roughness defined by  $Z_s = H_{rms}/L$  ( $L$  is the correlation length) is estimated with an RMSE of 0.08 cm for  $Z_s$ -values between 0.075 and 0.75 cm.

The objective of this study is to investigate the potential of Sentinel-1 C-band SAR data in VV polarization for estimating the soil roughness over bare agricultural soils. An inversion technique based on the use of neural networks (NNs) is used. The training of NNs is performed by using radar backscattering coefficients simulated through the Integral Equation Model (IEM). The performance of the inversion technique is then validated using both synthetic and real dataset. The real dataset is composed of Sentinel-1 images and ground measurements of soil moisture and surface roughness, collected in France and in Tunisia. Section 2 describes the inversion methodology, the neural networks, and datasets used (synthetic and real). The results and discussion are provided in Section 3. Finally, Section 4 presents the main conclusions.

## 2. Methods and Materials

### 2.1. Methodological Overview

An approach based on neural networks was chosen to estimate the soil roughness from Sentinel-1 images (SAR data) over bare agricultural soils at high spatial resolution “HSR” (plot scale or finer scale). This approach consisted of applying two networks one after the other, the first to estimate soil moisture and the second to estimate soil roughness. El Hajj et al. [19] showed that the use of VV alone provides better soil moisture estimation in comparison with the use of VH alone or the use of VV and VH together. Accordingly, only the VV polarization was used in this study for estimating soil parameters. In order to improve soil parameters estimates, a priori knowledge about soil moisture was introduced. Baghdadi et al. [15] showed that the use of a priori knowledge on soil moisture (dry to slightly wet or very wet information) improves soil moisture estimates. The a priori information on the moisture volumetric content “*mv*” was provided by an expert when using meteorological data (precipitations, temperature).

Three neural networks were developed for estimating *mv*, with and without a priori information on the soil moisture status:

- Case 1: No a priori information is available on the soil moisture status. In this case *mv* is estimated between 2 and 40 vol. %.
- Case 2: A priori information is available on *mv*. The soil is supposed to be dry to slightly wet according to expertise based mainly on meteorological data (precipitations, temperature). Soil moisture values are assumed to range from 2 to 25 vol. %.
- Case 3: A priori information is available on *mv*. The soil is supposed to be very wet according to expertise based on meteorological data. *mv*-values are assumed to vary between 25 and 40 vol. %.

The three NNs use the backscattering coefficient in VV polarization and the incidence angle as input. The output is only the soil moisture *mv*. In the two cases with a priori information on *mv*, an overlapping of 10 vol. % on *mv* was used between the datasets used for the training of these two networks. For dry to slightly wet soils, *mv*-values used for the training range from 2 to 30 vol. %. In the case of very wet soils, the *mv*-values vary between 20 and 40 vol. %.

Next, soil roughness could be estimated at a fine spatial scale (plot or sub-plot scale) using the soil moisture *mv* estimated by the first network. The standard acquisition mode of Sentinel-1 corresponds to acquisitions in both VV and VH polarizations. Since the VH polarization produces low signal levels over bare soils and is strongly affected by noise (radiometric accuracy is about 1.0 dB ( $3\sigma$ ) for VH [20]), it is less commonly used for the analysis of surface parameters. Accordingly, only VV was used. The NN for estimating soil roughness used the backscattering coefficient in VV, the incidence angle and the estimated soil moisture as input. The output was the soil surface roughness *Hrms*. The validation of the NN was carried out using, as input to the NN, the soil moisture estimated without and with a priori information on *mv*.

## 2.2. Artificial Neural Networks (Ann)

Multi-Layer Perceptron (MLP) neural networks were here developed to estimate soil parameters over bare agricultural soils (moisture content and roughness). Neural networks (NN) were trained using the Levenberg-Marquardt algorithm [21]. The neural network developed for estimating soil moisture has two hidden layers while the network built for estimating soil roughness has only one hidden layer. For each hidden layer, the number of neurons was determined by training the networks in order to obtain a good estimate of parameters while keeping a reasonable computing time. A number of 20 neurons was used [15]. For soil moisture estimation, two transfer functions were used, the first is Linear and the second is Tangent-Sigmoid. The transfer function used for the estimation of the surface roughness is Log-Sigmoid.

The most common approach for training neural networks consists of using a synthetic dataset generated from either physical or empirical radar backscattering model [10,17,22,23]. Training is accomplished to minimize the mean square error between the predicted NN outputs and the reference values.

## 2.3. Dataset Description

Neural networks were trained using the synthetic dataset generated from the radar backscattering model IEM (Integral Equation Model) with the range of surface roughness and soil moisture encountered in agricultural environments. The performance of inversion approaches for retrieving soil parameters is first validated by using another synthetic dataset that was different from the dataset used for NN learning. The validation was then performed using a real dataset composed of Sentinel-1 images collected over two contrasted agricultural study sites, one in France and one in Tunisia.

The inversion accuracy was evaluated through two statistical indexes: Bias (difference between estimated and measured variable) and Root Mean Square Error (RMSE).

### 2.3.1. Synthetic Dataset

In this study, the Integral Equation Model (IEM) developed by [8] and later modified by Baghdadi et al. [24,25] was used for modeling the radar backscattered signal as a function of soil parameters. This physical model is widely used to estimate soil moisture [10,15,17].

The radar backscattering coefficient that depends of soil moisture and surface roughness (in addition to SAR instrumental parameters) was simulated using the IEM calibrated by Baghdadi et al. [24,25]. This calibration consisted of replacing the measured correlation length by a fitting parameter ( $L_{opt}$ ) that depends on the root mean square surface height ( $H_{rms}$ ) and the SAR parameters (radar incidence angle, and radar frequency). The use of the fitting parameter ( $L_{opt}$ ) in the IEM model instead of the correlation length leads to an extension of the IEM's theoretical validity domain for HH and VV polarizations from  $H_{rms} \leq 3$  cm (C-band) to  $H_{rms} \leq 5.1$  cm [24,26]. For the HV polarization, the IEM ensures correct physical behaviour to approximately  $H_{rms} = 3.8$  cm (C-band) [25]. In the C-band, the fitting parameter  $L_{opt}$  was defined for each polarization follows:

$$L_{opt}(H_{rms}, \theta, VV) = 1.281 + 0.134(\sin 0.19\theta)^{-1.59} \times H_{rms} \quad (1)$$

where  $\theta$  is the incidence angle expressed in degrees, and  $L_{opt}$  and  $H_{rms}$  are expressed in cm. The formulations for  $L_{opt}$  were obtained with a Gaussian correlation function.

The IEM was used to generate a synthetic dataset of backscattering coefficients in VV polarization ( $\sigma^\circ VV$ ) from a wide range of  $\theta$  (20° to 45°),  $mv$  (2 to 40 vol. %), and  $H_{rms}$  (0.5 to 3.8 cm). An element of this dataset is a vector composed of a combination of three parameters  $\theta$ ,  $mv$ ,  $H_{rms}$ , and simulated  $\sigma^\circ VV$ . Each input vector to the IEM ( $\theta$ ,  $mv$ ,  $H_{rms}$ ) is generated using a pseudorandom function in order to cover the range of each input parameter [17]. In the modified IEM model, the empirical model developed by Hallikainen et al. [27] was used to derive the dielectric constant from the surface volumetric soil moisture content and soil texture.

A total of 9360 elements corresponding to 18 surface roughness values ( $rms$  between 0.5 and 3.8 cm), 20 soil moisture values ( $mv$  between 2 and 40 vol. %, 26 radar incidence angles ( $\theta$  between  $20^\circ$  and  $45^\circ$ ) was considered. In order to make the IEM simulations more realistic, Sentinel-1 radiometric error was added to simulated backscattering coefficients. In Schwerdt et al. [20], this error is about 0.70 dB ( $3\sigma$ ) for VV polarization. Accordingly, zero-mean Gaussian random noise with a standard deviation of  $\pm 0.70$  dB was added to simulated backscattering coefficients in VV polarization. In order to obtain a statistically significant dataset, 100 noise samples were generated for the simulated backscattering coefficients of each element of the dataset. Finally, the synthetic dataset was randomly divided into equal amounts, where 50% of the synthetic dataset was used for training the neural networks, and the remaining 50% served for validation.

### 2.3.2. Real Dataset

An experimental dataset was also used in this study, consisting of Sentinel-1 images as well as ground measurements of soil moisture and surface roughness collected over two agricultural study sites: one in France and one in Tunisia (Figure 1, Table 1). Sentinel-1 images (C-band, radar wavelength about 5.6 cm) were acquired with incidence angles between  $34^\circ$  and  $41^\circ$ , and in VV polarization.

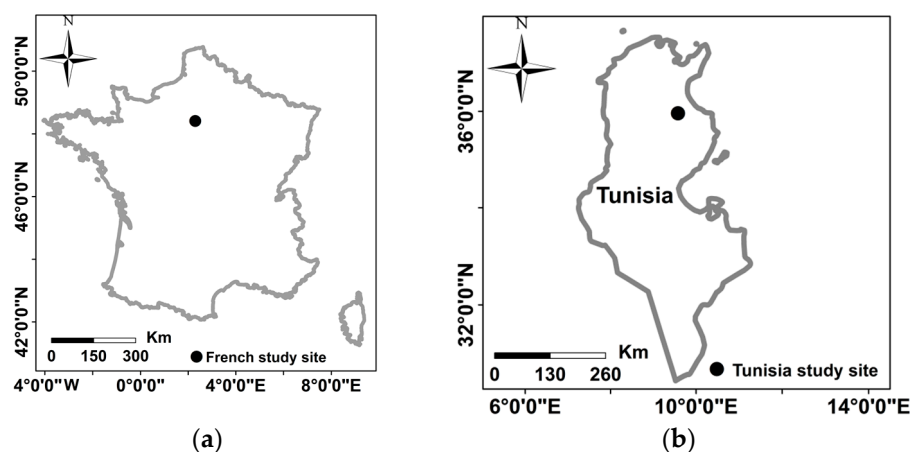


**Figure 1.** Location of our two study sites: Versailles plain (a) and Kairouan plain (b).

**Table 1.** Description of the real dataset used in this study for validating the inversion approach.

Site	SAR Sensor	Incidence Angle ( $^\circ$ )	Dates (Day/Month/Year)	Number of Data
French site	Sentinel-1	$\sim 37^\circ$	15/3/2017; 27/3/2017 2/4/2017; 8/4/2017	24 measurements
Tunisian site	Sentinel-1	$\sim 39^\circ$ to $41^\circ$	18/12/2015; 4/2/2016 3/4/2016; 4/4/2016 23/12/2016; 5/1/2017 9/2/2017	85 measurements

### Study Sites

The French study site is the Versailles plain. It is located west of Paris and covers about 221 km<sup>2</sup> ( $48^\circ 46' - 48^\circ 56' N$ ;  $1^\circ 50' - 2^\circ 07' E$ , Figure 1) [28]. This agricultural peri-urban site is characterized by a semi-oceanic climate with an average rainfall of 570 mm/year and an average annual temperature of 11.3  $^\circ C$  (INRA meteorological station of Thiverval-Grignon, 1986–2016). Rainfed annual crop systems cover 99 km<sup>2</sup> and develop over two embedded plateaus, and also over the gentle slopes at their edges and the valleys at their bottom. The main crop rotations in the area involve winter wheat, winter rapeseed, winter and spring barley and maize on occasion [28]. Conventional tillage practices are



used: ploughing in November–December, followed by chisel in March then seedbed preparation for spring cereals (spring barley in March, maize in April). The main cultivated soils according to the The Food and Agriculture Organization of the United Nations (FAO) classification (World Reference Base (WRB) [28] are haplic or glossic luvisols deriving from loessic material over the plateaus, calcareous cambisols deriving from limestones and/or colluvic material and/or chalk along slopes and stagnic colluvic cambisols in the valley bottoms. The topsoil texture is dominated by silt loam (silt > 50%) with extreme textural classes varying from sandy loam to silty clay. The clay content is between 14% and 32% (22% in median). The Tunisian study site is situated in the Kairouan plain, in central Tunisia (35°1′–35°55′ N–9°23′–10°17′ E, Figure 1). The climate in this region is semi-arid Mediterranean, with an average rainfall of approximately 300 mm/year, characterized by a rainy season lasting from October to May, with the two rainiest months being October and March [29]. The study site consists mainly of agricultural fields (cereals) on flat landscape. Soil texture measurements showed a clay percentage between 2.4% and 53.1% and sand percentage between 4.4% and 84.3% [29].

### SAR Satellite Images

Four Sentinel-1 images were acquired in March and April 2017 (Table 1) over the French study site. In addition, 7 Sentinel-1 images acquired over the Kairouan plain between 2015 and 2017 were used in this study. All Sentinel-1 images acquired with a spatial resolution of 10 m and in VV polarization were radiometrically calibrated in order to convert their digital numbers into radar backscattering coefficients.

### In Situ Measurements

Simultaneously with the Sentinel-1 acquisitions, in situ measurements of soil moisture and surface roughness were collected on several reference bare plots of a few hectares. Soil moisture was determined gravimetrically at each reference plot of the French site in using soil samples collected within cylinders of 528 cm<sup>3</sup> between 0 and 8 cm depth (2–7 measures by plot). For the Tunisian site, between 20 and 30 volumetric soil moisture measurements (*mv*) were performed in the first top 5 cm using calibrated TDR (Time Domain Reflectometry) probes. The mean volumetric soil moisture was then calculated for each reference plot and each date. The soil moisture on the reference plots ranged between 14 and 24 vol. % for the French site and between 5 and 42 vol. % for the Tunisian site.

The soil roughness measurements made in Tunisia on the reference plots used 1 m long pin profiler with a resolution of 2 cm. Ten roughness profiles (five parallel and five perpendicular to the tillage row direction) were made in each reference field using a 1 m long needle-profilometer and a sampling interval of 2 cm. From these roughness profiles, the root mean square surface height (*Hrms*) was then calculated for each reference plot using the mean of all autocorrelation functions acquired for each reference plot. For the French site, soil roughness was estimated with a fully automatic photogrammetric method [30]. The rms surface height ranged between 0.56 cm and 4.55 cm for the reference plots in the Tunisian site and between 0.41 cm and 2.90 cm for the reference plots in the French site.

Finally, each element of our real dataset was composed of in situ measurements (*mv* and *Hrms*) and Sentinel-1 information (mean of radar backscattered coefficients in VV, and radar incidence angle). For each reference plot, the mean of radar backscattered coefficients was calculated by averaging the values of all pixels within the reference plot.

## 3. Results and Discussion

The different neural networks were tested for the evaluation of the accuracy of soil roughness estimates using synthetic and real datasets.

### 3.1. Synthetic Dataset

The estimation of soil roughness ( $H_{rms}$ ) requires the use of an estimate of  $mv$ . First, we will discuss the performance of networks developed for the estimation of  $mv$ . Then, the network built for estimating  $H_{rms}$  is analyzed.

#### 3.1.1. Estimation of $mv$

For more details on the networks used for estimating  $mv$ , readers can refer to [19]. In El Hajj et al. [19], VV polarization provides better results in comparison to VH alone or to the use of VV and VH together. Only the results corresponding to VV are therefore presented.

##### Case 1: No a Priori Information on the Soil Moisture State

In this case,  $mv$  is supposed between 2 and 40 vol. %. The RMSE of the  $mv$  estimates is of 4.9 vol. % for  $mv$  between 2 and 25 vol. % and 6.6 vol. % for  $mv$  between 25 and 40 vol. %. An overestimation of 2.4 vol. % on  $mv$  is observed for  $mv$  between 2 and 25 vol. %, and an underestimation of  $-3.8$  vol. % is obtained for  $mv$  between 25 and 40 vol. %. For the entire range of  $mv$ , between 2 and 40%, the RMSE of  $mv$  is of 5.7 vol. %.

Next, the performance of the algorithm is analyzed according to  $H_{rms}$  and incidence angle " $\theta$ " (Figure 2a,b). Results show that the bias (estimated  $mv$ –measured  $mv$ ) and the RMSE are strongly dependent on  $H_{rms}$ . The RMSE of  $mv$  in the case of inversion without a priori information on  $mv$  increases from 4.0 vol. % for  $H_{rms} = 0.5$  cm to 7.2 vol. % for  $H_{rms} = 3.8$  cm for  $mv$  between 2 and 25 vol. % (dry to slightly wet soils). Under very wet soil conditions, the RMSE of  $mv$  decreases from 11.7 vol. % for  $H_{rms} = 0.5$  cm to 4.0 vol. % for  $H_{rms} = 3.8$  cm. The high RMSE values in the case of dry to slightly wet conditions and high  $H_{rms}$ -values are due to an overestimation of  $mv$  (bias increases from  $-2.7$  to  $+6.1$  vol. % for  $H_{rms}$  between 0.5 and 3.8 cm). Similarly, the high RMSE values in the case of very wet conditions and low  $H_{rms}$ -values are due to an underestimation of  $mv$  (bias increases from  $-10.5$  to 0 vol. % for  $H_{rms}$  between 0.5 and 3.8 cm).

In addition, results show that the RMSE of  $mv$  slightly depends on  $\theta$  in the case of no a priori information on  $mv$  (Figure 2c,d). The RMSE is about 4.9 vol. % for dry to slightly wet soil conditions and about 6.5 vol. % for very wet soils. The overestimation of  $mv$  in dry to slightly conditions is approximately 2.5 vol. % for  $\theta$  between  $20^\circ$  and  $45^\circ$ . For very wet soil conditions, the underestimation of  $mv$  is about  $-3.8$  vol. % for  $\theta$  between  $20^\circ$  and  $45^\circ$ .

##### Case 2: A Priori Information on $mv$ : Dry to Slightly Wet Soils (2 to 25 vol. %)

In this case the NN was trained using synthetic dataset with  $mv$  between 2 and 30 vol. %. Its validation was done using the validation synthetic dataset with  $mv$  between 2 and 25 vol. %. Results show that the introduction of a priori information on  $mv$  in the case of dry to slightly wet soil conditions improves the  $mv$  estimates. The RMSE of  $mv$  estimates decreases from 4.9 vol. % without a priori information on  $mv$  to 3.6 vol. % in the case of a priori information on  $mv$ . In addition, the difference between estimated and measured  $mv$  is also reduced from 2.4 vol. % to 1.1 vol. %.

This improvement of the estimation quality is also well observed when the accuracy of  $mv$  estimates is analyzed according to  $H_{rms}$  and  $\theta$ . The RMSE of  $mv$  estimates varies between 4.2 and 4.8 vol. % for all  $mv$  and  $H_{rms}$  values considered in this study. The bias was also reduced with values between  $-3.0$  vol. % (low  $H_{rms}$ ) and  $+4.0$  vol. % (high  $H_{rms}$ ). Finally, RMSE and bias on  $mv$  estimates are slightly dependent on the incidence angle.

##### Case 3: A Priori Information on $mv$ : Very Wet Soils (25 to 40 vol. %)

In this case the NN was trained using synthetic dataset with  $mv$  between 20 and 40 vol. %. Its validation was made using the validation synthetic dataset with  $mv$  between 25 and 40 vol. %. Results show that the use of a priori information on  $mv$  in the case of very wet soil conditions improves the  $mv$  estimates

(Figure 2c,d). The RMSE of  $mv$  estimates decreases from 6.6 vol. % without a priori information on  $mv$  to 5.0 vol. % in the case of a priori information on  $mv$ . In addition, the difference between estimated and measured  $mv$  is also well reduced from  $-3.8$  vol. % to  $-2.3$  vol. %. According to  $Hrms$ , the RMSE of  $mv$  estimates varies between 3.9 and 7.0 vol. % for all  $mv$  and  $Hrms$  values of the validation synthetic dataset (case of very wet conditions). The highest RMSE-values correspond to low  $Hrms$ -values. The bias is also well reduced mainly for low  $Hrms$ -values (by a factor 2). The analysis of the RMSE and the bias shows relatively close values according to the incidence angle.

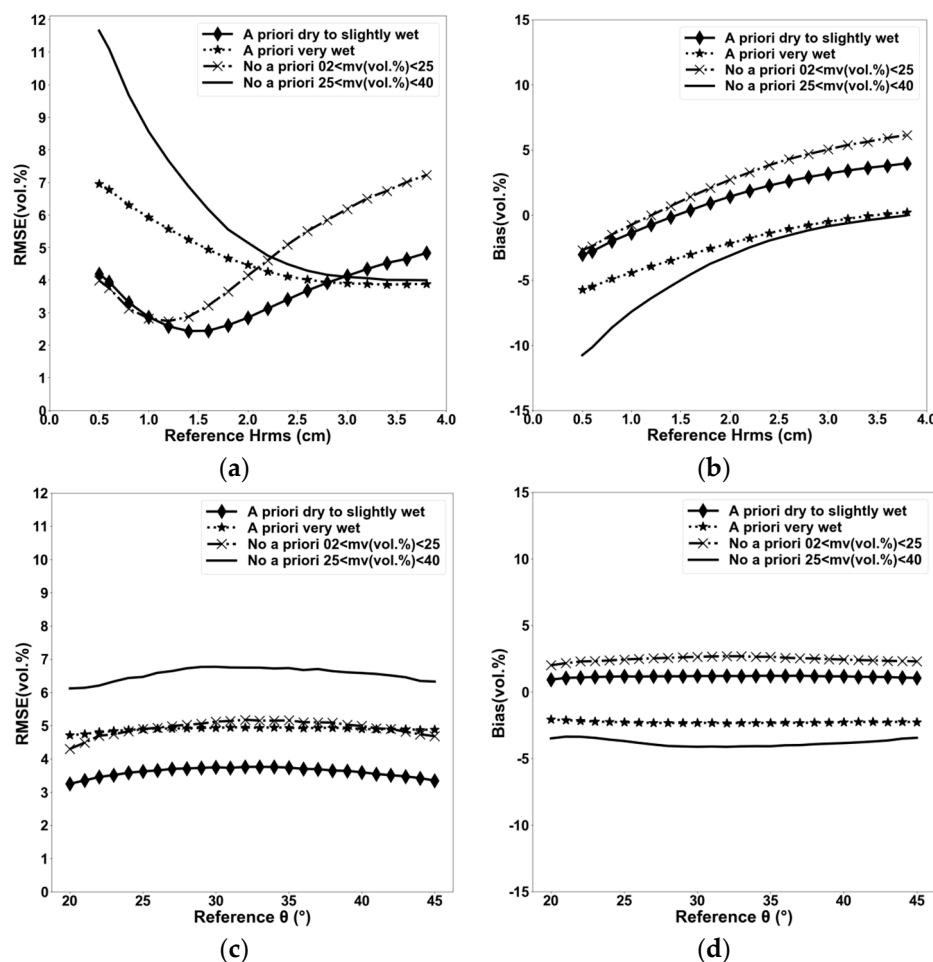


**Figure 2.** Accuracy of the  $mv$  estimates (RMSE and Bias “=estimated – measured”) retrieved from the synthetic dataset in VV polarization. Three NNs are tested: without a priori information on  $mv$  (case 1), with a priori information on  $mv$  with dry to slightly wet soil conditions (case 2), with a priori information on  $mv$  with very wet conditions (case 3). (a) RMSE of  $mv$  according to  $Hrms$ ; (b) Bias on  $mv$  estimates according to  $Hrms$ ; (c) RMSE of  $mv$  according to  $\theta$ ; (d) Bias on  $mv$  estimates according to  $\theta$ .

## Discussion

The use of a priori information on  $mv$  strongly improves the estimate of  $mv$ . For the range of surface roughness most encountered in agricultural environments with  $Hrms$  between 1 and 2 cm, the RMSE of  $mv$  is lower than 6 vol. % (varies between 2.4 and 5.9 vol. %). The difference between estimated and real  $mv$  varies between  $-1.4$  and  $+1.4$  vol. % in the case of dry to slightly wet soils. An underestimation of  $mv$  from  $-4.4$  to  $-2.2$  vol. % in the case of very wet soils is observed for  $Hrms$  between 1 and 2 cm.



### 3.1.2. Estimation of $H_{rms}$

The estimation of the soil roughness is carried out after a first step which consisted of estimating  $mv$  because the network which estimates  $H_{rms}$  needs  $mv$ -values as input. These are the  $mv$  estimated by the previous networks built to estimate  $mv$  which are used (no a priori information and a priori information on  $mv$ ). In addition to these cases corresponding to operational conditions for estimating the soil roughness, the case where the  $mv$  used as input to the network corresponds to exact  $mv$  without estimation error ( $mv$ -values of the validation synthetic dataset) is also tested.

Figure 3 shows the results of the inversion of the radar signal for estimating soil roughness. Results show better estimates of  $H_{rms}$  when the  $mv$  used at the input of the NN corresponds to the synthetic  $mv$  (RMSE = 0.71 cm). The results obtained using the  $mv$  estimated without and with a priori information on  $mv$  are of poor accuracy with RMSE of 1.01 cm and 0.94 cm, respectively. This shows that the use of  $mv$  estimates with an accuracy of about 6 vol. % is not sufficient to accurately estimate the soil roughness in C-band and VV polarization. In addition, Figure 3 shows an overestimation of  $H_{rms}$  for low  $H_{rms}$ -values and an underestimation of  $H_{rms}$  for  $H_{rms}$  higher than 2 cm.

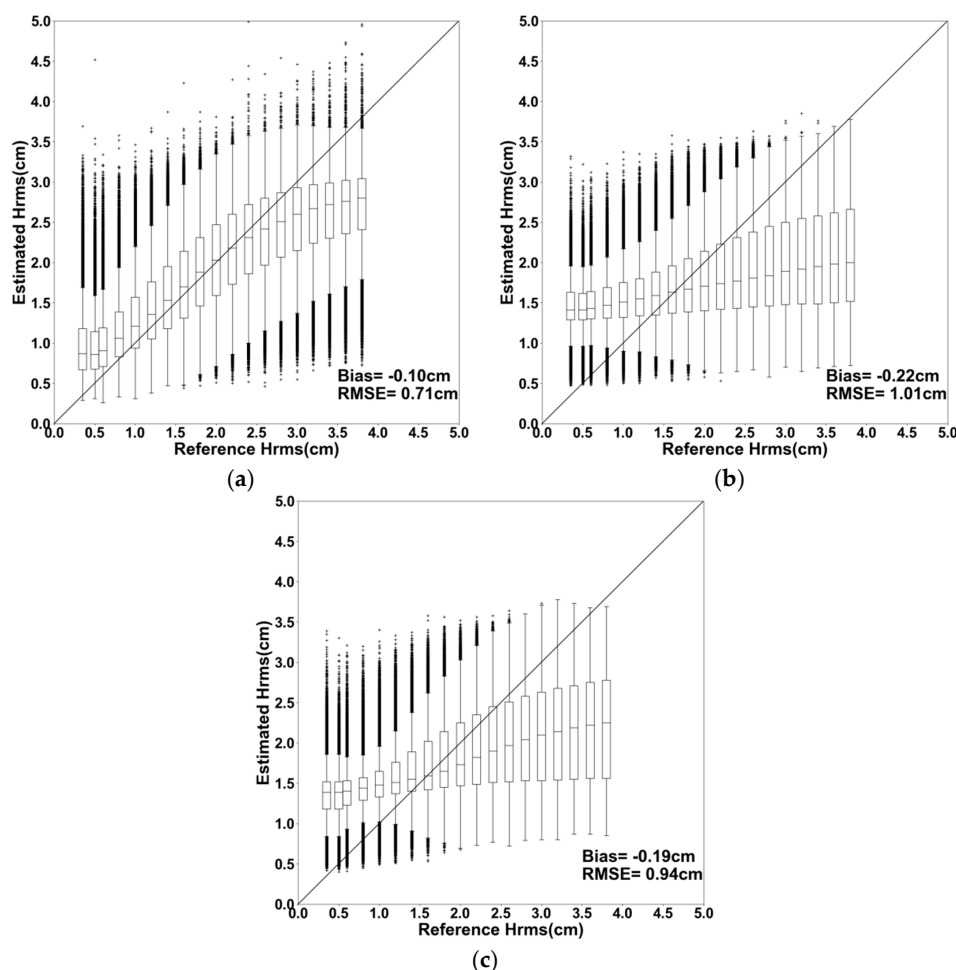


**Figure 3.** Box plots of  $H_{rms}$  (cm) retrieved from the synthetic dataset using VV polarization. (a) the input  $mv$  to the network corresponds to synthetic  $mv$  (those that are in the validation synthetic dataset, without error on  $mv$ ); (b) the input  $mv$  to the network corresponds to  $mv$  estimated by the NN built for estimating  $mv$  without a priori information on  $mv$  (case 1); (c) the input  $mv$  to the network corresponds to  $mv$  estimated by the NN built for estimating  $mv$  with a priori information on  $mv$  (cases 2 and 3).

The performance of the neural network is also studied as a function of  $mv$  and the incidence angle ( $\theta$ ) only when the  $mv$  in input to the NN corresponds to the synthetic  $mv$  (without estimation error)

(Figure 4). The RMSE of  $H_{rms}$  decreases from 0.80 cm for  $mv = 2$  vol. % to 0.70 cm for  $mv$  higher than 15 vol. %. In addition, the RMSE of  $H_{rms}$  decreases when the incidence angle increases. The RMSE of  $H_{rms}$  shows values between 0.90 cm for  $\theta = 20^\circ$  and 0.60 cm for  $\theta = 45^\circ$ . This is due to the sensitivity of radar signal to  $H_{rms}$ , which is much stronger for high values of  $\theta$  than for low values of  $\theta$  [5]. Finally, a slight under-estimation of reference  $H_{rms}$ -values (bias about  $-0.1$  cm) was observed for all  $mv$  and  $\theta$  values (Figure 4).

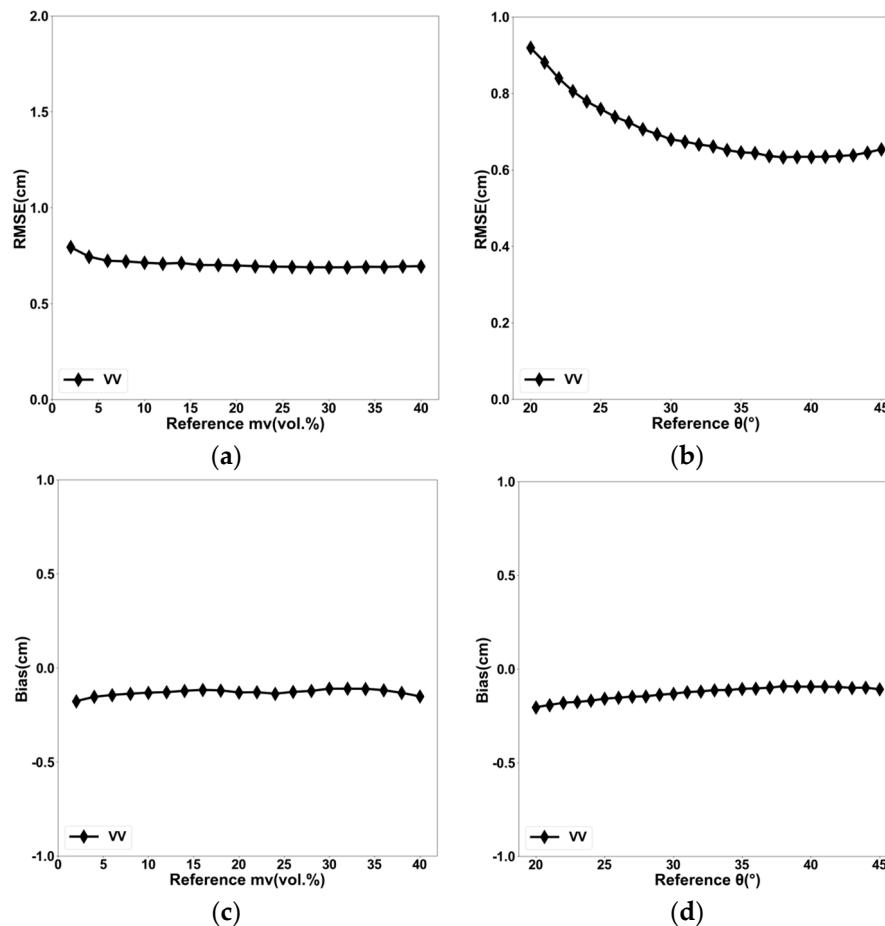


**Figure 4.** Accuracy of the  $H_{rms}$  estimates (RMSE) as a function of the soil moisture and the incidence angle. The  $mv$ -values as input to the network correspond to exact  $mv$  (those that are in the validation synthetic dataset). (a) RMSE of  $H_{rms}$  according to  $mv$ ; (b) RMSE of  $H_{rms}$  according to  $\theta$ ; (c) Bias on  $H_{rms}$  estimates according to  $mv$ ; (d) Bias on  $H_{rms}$  estimates according to  $\theta$ .

### 3.2. Real Dataset

The NNs built for estimating  $mv$  and  $H_{rms}$  are then analyzed using the real Sentinel-1 dataset. Figure 5 gives the results obtained for the estimation of  $mv$ . Results show that the introduction of a priori information on  $mv$  provides better accuracy of the  $mv$  estimates than the case without a priori information on  $mv$  (RMSE = 6.0 vol. % with a priori on  $mv$  and RMSE = 6.9 vol. % without a priori on  $mv$ ). The analysis of the difference between the estimated and measured  $mv$  shows that the strong underestimates of the  $mv$  corresponds to low  $H_{rms}$ -values ( $H_{rms} < 2$  cm) and the strong overestimates corresponds to high  $H_{rms}$ -values ( $H_{rms} > 2$  cm).

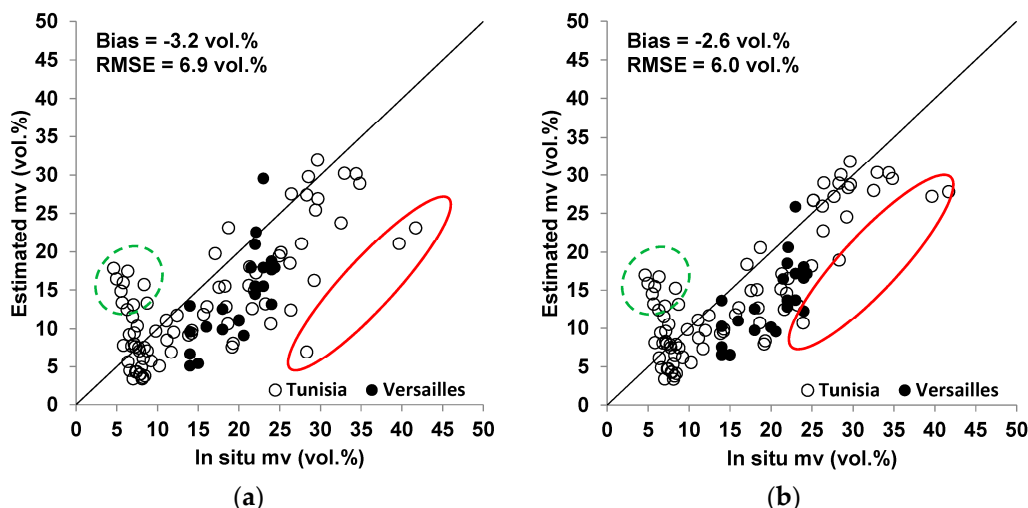


**Figure 5.** Retrieved  $mv$  versus in situ measurements. (a) using VV without a priori information on  $mv$ ; (b) using VV with a priori information on  $mv$ . Each point corresponds to one reference plot. The red ellipse represents reference plots with low  $Hrms$ -values ( $Hrms < 2$  cm). The green dashed ellipse represents reference plots with high  $Hrms$ -values ( $Hrms > 2$  cm).

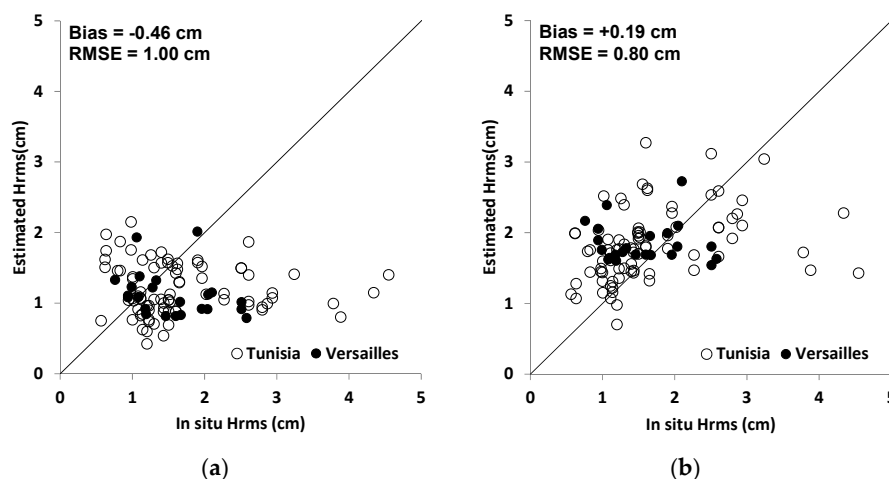
Next, the soil roughness is estimated using the soil moisture provided by the  $mv$ -network. Two approaches are tested. The first one uses as input to the  $Hrms$ -network the  $mv$  estimated at high spatial resolution “HSR” (plot scale). The second one uses as input to the  $Hrms$ -network the average soil moisture estimated by the  $mv$ -network at the study site scale (an area of a few  $km^2$ ) using the mean backscattering coefficient of all bare agricultural pixels. This second approach assumes that the soil moisture is of the same order for all bare agricultural plots located in the area under consideration (no irrigation activities and similar soil composition). The use of  $mv$  estimated at the scale of the study site in the estimation technique of  $Hrms$  could be relevant only when the study site is not irrigated (case of Versailles site). Indeed, if the SAR images are acquired during the dry season with irrigation activities on the study site, the use of an average soil moisture estimated at the scale of the study site (average  $mv$  calculated on all the bare soil agricultural plots) will lead to a strong overestimation of  $Hrms$  since the  $mv$  used for irrigated plots in the neural network for estimating  $Hrms$  will most probably be underestimated.

Figure 6 shows the results of the estimation of  $Hrms$  using the two inversion configurations described before:

- At the input of the network for the estimation of  $Hrms$ , the  $mv$  used corresponds to  $mv$  estimated at plot scale (using the mean radar signal calculated by averaging for each reference plot the values of all pixels within the reference plot).
- At the input of the network for the estimation of  $Hrms$ , the  $mv$  used corresponds to  $mv$  estimated at the scale of the study site (using the mean radar signal calculated by averaging the values of all bare soil pixels within the study site).

For these two configurations, a priori information on  $mv$  is used in the network for estimating  $mv$ .

Results show that the accuracy of the estimates of  $Hrms$  is similar in using the  $mv$  estimated at the study site scale (a few tens of  $km^2$ ) than when using the  $mv$  estimated at the plot scale. The RMSE is 0.80 cm when the  $mv$  used corresponds to  $mv$  estimated at the scale of the study site and 1.00 cm when the  $mv$  is estimated at the plot scale (Figure 6).



**Figure 6.** Retrieved *Hrms* versus measured measurements. (a) the *mv* used at the input of the network corresponds to *mv* estimated at the plot scale; (b) the *mv* used at the input of the network corresponds to *mv* estimated at the scale of the study site. For these two configurations, a priori information on *mv* was used for estimating *mv*.

Figure 6 shows also that the estimation of *Hrms* is very difficult for high roughness values (*Hrms* > 3 cm). Indeed, the radar signal in C-band is highly sensitive to the soil roughness for *Hrms* values lower than 2 cm [10]. Beyond 3 cm, the radar signal tends to saturate with the *Hrms*. For soil roughness lower than 3 cm, the precision (RMSE) of the soil roughness estimates is of 0.65 cm when the *mv* used at the input of the network corresponds to *mv* estimated at the scale of the study site.

In a recent study, Bousbih et al. [31] investigate the sensitivity of the Sentinel-1 radar signal to soil moisture and surface roughness. For a bare soil, results showed that the radar signal in the C-band increases as soil moisture increases (5 vol. % < *mv* < 35 vol. %) with a sensitivity of 0.27 dB/vol. % and 0.18 dB/vol. % for VV and VH, respectively. In addition, the Sentinel-1 signal increases about 5 dB for VV polarization and 4 dB for VH polarization as the soil roughness increases from 0.5 cm to 3 cm. Beyond 3 cm, the radar signal tend to saturates with increasing soil roughness.

#### 4. Conclusions

The objective of this study was to investigate the potential of the C-band in VV polarization for estimating the soil roughness over bare agricultural areas using the neural network technique. Neural networks (NNs) were trained with radar backscattering coefficients generated from the Integral Equation Model (IEM). A second simulated dataset and a real dataset composed of Sentinel-1 images were then used to analyze the performance of the inversion technique.

The inversion procedure of the soil roughness involves two steps. The first one consists of the estimation of the soil moisture. Results show that the soil moisture could be estimated with an RMSE better than 6 vol. % when a priori information on *mv* is used in the neural network. The second neural network uses this estimation of *mv* in order to estimate the soil roughness at the plot scale. Results obtained show estimates of *Hrms* with an RMSE of 0.94 cm. This accuracy of *Hrms* obtained in using the NN built with a priori information on *mv* shows that the use of *mv* estimates with an accuracy of about 6 vol. % is not sufficient to accurately estimate the soil roughness in the C-band and VV polarization. From the real dataset, results show that the accuracy of *Hrms* estimates in using the *mv* estimated at the study site scale is better than that using the *mv* estimated at the plot scale, with an RMSE of *Hrms* about 0.80 cm (RMSE = 1.00 cm using *mv* estimated at the plot scale). The use of *mv* estimated at the scale of the study site is possible only when the study site is not irrigated.

This first study on the potential of Sentinel-1 data for estimating the soil roughness shows that the development of an automatic and generalizable inversion procedure of the C-band radar signal

does not allow a pertinent estimation of the soil roughness. The accuracy of soil roughness estimates obtained in this study cannot satisfy the requirements of operational users of soil roughness products (in particular to modelers) because the need is at least three roughness classes: smooth (sowing), medium (small plowing) and rough (large plowing).

Only methods based on the use of experimental relationships, which are often difficult to apply to sites other than those for which they were developed and are generally valid only for specific soil conditions, allows the mapping of three roughness classes [5]. Indeed, different experimental studies have revealed that the sensitivity of the radar signal to surface roughness (i.e., the slope of the regression lines) can be highly variable from one site to another. In addition, the experimental relationships between the radar signal and *Hrms* are established for a given incidence angle and a range of soil moisture. The soil composition could also be different from one site to another. All these reasons explain why the experimental relationships are not generalizable.

**Acknowledgments:** This research was supported by IRSTEA (National Research Institute of Science and Technology for Environment and Agriculture) and the French Space Study Center (CNES, DAR 2017 TOSCA). The authors wish to thank the European Commission and the European Space Agency (ESA) for kindly providing the Sentinel-1 images. The authors wish to thank Dalila Hadjar and Safa Bousbih for their support during the field campaigns.

**Author Contributions:** Nicolas Baghdadi, Mohammad El Hajj and Mohammad Choker conceived and designed the experiments; Mohammad El Hajj and Mohammad Choker performed the experiments; Nicolas Baghdadi, Mohammad El Hajj, Mohammad Choker, Mehrez Zribi, Hassan Bazzi, Emmanuelle Vaudour, Jean Marc Gilliot and Dav M. Ebengo analyzed the data; Nicolas Baghdadi wrote the paper.

**Conflicts of Interest:** The authors declare no conflict of interest.

## References

- Ogilvy, J.A.; Merklinger, H.M. Theory of wave scattering from random rough surfaces. *J. Acoust. Soc. Am.* **1991**, *90*, 3382. [[CrossRef](#)]
- Baghdadi, N.; Choker, M.; Zribi, M.; Hajj, M.E.; Paloscia, S.; Verhoest, N.E.; Lievens, H.; Baup, F.; Mattia, F. A new empirical model for radar scattering from bare soil surfaces. *Remote Sens.* **2016**, *8*, 920. [[CrossRef](#)]
- Zribi, M.; Gorraeb, A.; Baghdadi, N. A new soil roughness parameter for the modelling of radar backscattering over bare soil. *Remote Sens. Environ.* **2014**, *152*, 62–73. [[CrossRef](#)]
- Aubert, M.; Baghdadi, N.; Zribi, M.; Douaoui, A.; Loumagne, C.; Baup, F.; El Hajj, M.; Garrigues, S. Analysis of TerraSAR-X data sensitivity to bare soil moisture, roughness, composition and soil crust. *Remote Sens. Environ.* **2011**, *115*, 1801–1810. [[CrossRef](#)]
- Baghdadi, N.; King, C.; Bourguignon, A.; Remond, A. Potential of ERS and RADARSAT data for surface roughness monitoring over bare agricultural fields: Application to catchments in Northern France. *Int. J. Remote Sens.* **2002**, *23*, 3427–3442. [[CrossRef](#)]
- Baghdadi, N.; Zribi, M.; Loumagne, C.; Ansart, P.; Anguela, T.P. Analysis of TerraSAR-X data and their sensitivity to soil surface parameters over bare agricultural fields. *Remote Sens. Environ.* **2008**, *112*, 4370–4379. [[CrossRef](#)]
- Baghdadi, N.; Cerdan, O.; Zribi, M.; Auzet, V.; Darboux, F.; El Hajj, M.; Kheir, R.B. Operational performance of current synthetic aperture radar sensors in mapping soil surface characteristics in agricultural environments: Application to hydrological and erosion modelling. *Hydrol. Process.* **2008**, *22*, 9–20. [[CrossRef](#)]
- Fung, A.K. *Microwave Scattering and Emission Models and Their Applications*; Artech House: Boston, MA, USA, 1994.
- Zribi, M.; Dechambre, M. A new empirical model to retrieve soil moisture and roughness from C-band radar data. *Remote Sens. Environ.* **2002**, *84*, 42–52. [[CrossRef](#)]
- Baghdadi, N.; Gaultier, S.; King, C. Retrieving surface roughness and soil moisture from SAR data using neural networks. In *Retrieval of Bio- and Geo-Physical Parameters from SAR Data for Land Applications*; ESTEC Publishing Division: Sheffield, UK, 2002; pp. 315–319.
- Ulaby, F.T.; Moore, R.K.; Fung, A.K. *Microwave Remote Sensing: Active and Passive, Vol. III, Volume Scattering and Emission Theory, Advanced Systems and Applications*; Artech House, Inc.: Dedham, MA, USA, 1986; pp. 1797–1848.



12. Holah, N.; Baghdadi, N.; Zribi, M.; Bruand, A.; King, C. Potential of ASAR/ENVISAT for the characterization of soil surface parameters over bare agricultural fields. *Remote Sens. Environ.* **2005**, *96*, 78–86. [[CrossRef](#)]
13. Aubert, M.; Baghdadi, N.N.; Zribi, M.; Ose, K.; El Hajj, M.; Vaudour, E.; Gonzalez-Sosa, E. Toward an Operational Bare Soil Moisture Mapping Using TerraSAR-X Data Acquired Over Agricultural Areas. *IEEE J. Sel. Top. Appl. Earth Obs. Remote Sens.* **2013**, *6*, 900–916. [[CrossRef](#)]
14. Baghdadi, N.; Camus, P.; Beaugendre, N.; Issa, O.M.; Zribi, M.; Desprats, J.F.; Rajot, J.L.; Abdallah, C.; Sannier, C. Estimating surface soil moisture from TerraSAR-X data over two small catchments in the Sahelian Part of Western Niger. *Remote Sens.* **2011**, *3*, 1266–1283. [[CrossRef](#)]
15. Baghdadi, N.; Cresson, R.; El Hajj, M.; Ludwig, R.; La Jeunesse, I. Estimation of soil parameters over bare agriculture areas from C-band polarimetric SAR data using neural networks. *Hydrol. Earth Syst. Sci.* **2012**, *16*, 1607–1621. [[CrossRef](#)]
16. El Hajj, M.; Baghdadi, N.; Zribi, M.; Belaud, G.; Cheviron, B.; Courault, D.; Charron, F. Soil moisture retrieval over irrigated grassland using X-band SAR data. *Remote Sens. Environ.* **2016**, *176*, 202–218. [[CrossRef](#)]
17. Paloscia, S.; Pettinato, S.; Santi, E.; Notarnicola, C.; Pasolli, L.; Reppucci, A. Soil moisture mapping using Sentinel-1 images: Algorithm and preliminary validation. *Remote Sens. Environ.* **2013**, *134*, 234–248. [[CrossRef](#)]
18. Zribi, M.; Chahbi, A.; Shabou, M.; Lili-Chabaane, Z.; Duchemin, B.; Baghdadi, N.; Amri, R.; Chehbouni, A. Soil surface moisture estimation over a semi-arid region using ENVISAT ASAR radar data for soil evaporation evaluation. *Hydrol. Earth Syst. Sci.* **2011**, *15*, 345–358. [[CrossRef](#)]
19. El Hajj, M.; Baghdadi, N.; Zribi, M.; Bazzi, H. Synergic use of Sentinel-1 and Sentinel-2 images for operational soil moisture mapping at high spatial resolution over agricultural areas. *Remote Sens.* **2017**, *9*, 1292. [[CrossRef](#)]
20. Schwerdt, M.; Schmidt, K.; Tous Ramon, N.; Klenk, P.; Yague-Martinez, N.; Prats-Iraola, P.; Zink, M.; Geudtner, D. Independent System Calibration of Sentinel-1B. *Remote Sens.* **2017**, *9*, 511. [[CrossRef](#)]
21. Marquardt, D.W. An algorithm for least-squares estimation of nonlinear parameters. *J. Soc. Ind. Appl. Math.* **1963**, *11*, 431–441. [[CrossRef](#)]
22. Notarnicola, C.; Angiulli, M.; Posa, F. Soil moisture retrieval from remotely sensed data: Neural network approach versus Bayesian method. *IEEE Trans. Geosci. Remote Sens.* **2008**, *46*, 547–557. [[CrossRef](#)]
23. Satalino, G.; Mattia, F.; Davidson, M.W.; Le Toan, T.; Pasquariello, G.; Borgeaud, M. On current limits of soil moisture retrieval from ERS-SAR data. *IEEE Trans. Geosci. Remote Sens.* **2002**, *40*, 2438–2447. [[CrossRef](#)]
24. Baghdadi, N.; Holah, N.; Zribi, M. Calibration of the integral equation model for SAR data in C-band and HH and VV polarizations. *Int. J. Remote Sens.* **2006**, *27*, 805–816. [[CrossRef](#)]
25. Baghdadi, N.; Chaaya, J.A.; Zribi, M. Semiempirical calibration of the integral equation model for SAR data in C-band and cross polarization using radar images and field measurements. *IEEE Geosci. Remote Sens. Lett.* **2011**, *8*, 14–18. [[CrossRef](#)]
26. Baghdadi, N.; Zribi, M. Characterization of Soil Surface Properties Using Radar Remote Sensing. In *Land Surface Remote Sensing in Continental Hydrology*; Elsevier: Amsterdam, The Netherlands, 2016; pp. 1–39.
27. Hallikainen, M.T.; Ulaby, F.T.; Dobson, M.C.; El-Rayes, M.A.; Wu, L.-K. Microwave dielectric behavior of wet soil-part 1: Empirical models and experimental observations. *IEEE Trans. Geosci. Remote Sens.* **1985**, *23*, 25–34. [[CrossRef](#)]
28. Vaudour, E.; Baghdadi, N.; Gilliot, J.-M. Mapping tillage operations over a peri-urban region using combined SPOT4 and ASAR/ENVISAT images. *Int. J. Appl. Earth Obs. Geoinform.* **2014**, *28*, 43–59. [[CrossRef](#)]
29. Gorraeb, A.; Zribi, M.; Baghdadi, N.; Mougenot, B.; Chabaane, Z.L. Potential of X-Band TerraSAR-X and COSMO-SkyMed SAR Data for the Assessment of Physical Soil Parameters. *Remote Sens.* **2015**, *7*, 747–766. [[CrossRef](#)]
30. Gilliot, J.-M.; Vaudour, E.; Michelin, J. Soil surface roughness measurement: A new fully automatic photogrammetric approach applied to agricultural bare fields. *Comput. Electron. Agric.* **2017**, *134*, 63–78. [[CrossRef](#)]
31. Bousbih, S.; Zribi, M.; Lili-Chabaane, Z.; Baghdadi, N.; El Hajj, M.; Gao, Q.; Mougenot, B. Potential of Sentinel-1 Radar Data for the Assessment of Soil and Cereal Cover Parameters. *Sensors* **2017**, *17*, 2617. [[CrossRef](#)] [[PubMed](#)]

